14th IEA Heat Pump Conference
15-18 May 2023, Chicago, Illinois

Long term performance analysis of a Dual-Source Heat Pump system by means of the Matlab/Simulink tool ALMABuild

Christian Natale*, Claudia Naldi, Matteo Dongellini, Gian Luca Morini

Department of Industrial Engineering, Alma Mater Studiorum – University of Bologna,
Viale del Risorgimento 2, Bologna 40136, Italy

Abstract

In this paper, the performance of a Dual-Source Heat Pump (DSHP), able to exploit energy from both air and ground, has been investigated through the Simulink toolbox ALMABuild. Two different control strategies for the external source selection have been implemented: with the first one, the ambient temperature is compared to a reference value (namely, switching temperature logic); with the second one, the heat pump is forced to operate in air-source mode and ground-source mode during the diurnal and the nocturnal hours, respectively (namely, scheduled times logic). The DSHP has been coupled to a building with unbalanced loads and to a Borehole Heat Exchanger (BHE) field, for which different total lengths of the borefield have been considered. The obtained results show that with undersized BHEs a DSHP achieves better annual performance with respect to Air-Source Heat Pumps (ASHPs) and Ground-Coupled Heat Pumps (GCHPs) coupled to the same borefield. In addition, a DSHP can reduce the ground temperature drift originated by undersized borefield and/or by unbalanced building loads. The paper shows how DSHPs can be selected for the replacement of traditional GCHPs in presence of undersized BHEs.

Selection and/or peer-review under the responsibility of the organizers of the 14th IEA Heat Pump Conference 2023.

Keywords: Dual-Source Heat Pump; Borehole Heat Exchangers; Annual Performance Factor; Matlab-Simulink; Control strategies.

1. Introduction

In the last decades the global energy demand, and consequently worldwide greenhouse gas emissions, has significantly increased in parallel with a better population wealth. In order to contrast climate change and simultaneously boosting its own energy security, the European Community is strongly promoting low carbon technologies [1-2]. In Italy, buildings account for about 30% of the total energy consumption [3] and, for this reason, the real estate industry must be involved in a systemic refurbishment. With this aim, the Italian government has granted state allowances to improve the building envelope thermal properties and the heating, ventilating and air conditioning (HVAC) systems [4].

Heat pumps are good candidates for this purpose since they strongly reduce the primary energy demand for space heating and cooling of buildings [5-6] if compared to traditional fossil fuel boilers. In fact, heat pumps are able to exploit significant shares of renewable energy from aerothermal, geothermal and hydrothermal energy sources [2]. In recent years, Air-Source Heat Pumps (ASHPs) have been the most sold units in Europe [1] thanks to the extremely wide source availability and low investment costs. However, the air-to-water heat pumps performance is deeply influenced by the external air temperature and, in particular, their efficiency decreases when the ambient temperature drops in winter and rises in summer, in correspondence of the largest building thermal load. Another drawback is related to the defrost cycles, which occur for heating operating mode when the ambient temperature is low and the relative humidity is high. The frost layer accumulated on the heat pump external heat exchanger can be removed with different techniques, such as the adoption of an

* Corresponding author. Tel.: +39-051-209-0467; fax: +39-051-209-0544.
E-mail address: christian.natale3@unibo.it.

electric resistance to melt the ice, the spray of hot water on the evaporator surface or the use of hot refrigerant by-passed from the compressor discharge port. Among defrost methodologies, the most widespread technique, used by commercial reversible heat pumps, is reverse cycle defrosting (RCD). For this reason, RCD has been considered in this paper as defrosting method [7].

On the contrary, Ground-Coupled Heat Pumps (GCHPs) performance is weakly influenced by the external air temperature. Indeed, starting from a depth of about ten meters the ground temperature is almost stable over the year and equal to the mean annual temperature of the locality. This circumstance, combined to a well-sized Borehole Heat Exchanger (BHE) field, guarantees that the GCHP annual efficiency is substantially higher than that of an ASHP [8]. The main drawback of GCHP systems is the high investment cost linked to the installation of BHEs, which requires an accurate analysis to avoid oversized borefields [9-10].

In order to reduce the BHE field length, guaranteeing high values of the heat pump seasonal performance factors, a Dual-Source Heat Pump (DSHP) able to exploit renewable energy from both air and ground can be adopted. In literature several studies have been carried out on multi-source heat pumps; however, they mostly considered multi-generator systems. Many authors [11-12] integrated solar collectors whilst others [13-14] combined photovoltaic/thermal solar panels to heat pump systems. In this work, only one heat generator has been considered, consisting in a multi-source heat pump prototype. This unit can exploit alternatively geothermal energy, by means of a BHEs field, and aerothermal energy, through a conventional finned tube heat exchanger. In this way, the heat pump can work in air-source mode when the ambient temperature is warmer, as during the milder part of the day, and operate in ground-source mode in the most severe part, avoiding the frost deposition and the consequent defrost cycle. Grossi et al. [15] conducted a preliminary analysis on the adoption of a DSHP similar to the one studied in this paper (i.e., a single unit able to exploit, alternately, air or ground as heat sources). In that work, the Authors utilized a commercial software for buildings dynamic simulation (Trnsys) and a single basic control strategy for the heat pump external source selection.

The aim of the present work is to evaluate the energy performance of a DSHP, comparing the overall efficiency achievable with this kind of unit with those of traditional systems, such as a ASHP and a GCHP. Seasonal and annual performance of these systems has been investigated coupling a BHE field having different sizes to the multi-source generator. By using ALMABuild [16-17], an open-source Matlab-Simulink toolbox, seven-year simulations have been performed to take into account the long-term effects of the ground exploitation on the soil temperature drift. Moreover, when the DSHP is considered as heat generator, two control strategies have been implemented to choose the heat pump external source. The former logic selects the operating heat source by comparing a reference temperature, namely the switching temperature, to the external air temperature. The latter logic considers daily scheduled times in which the external source of the DSHP is pre-defined independent of the climatic conditions. The simulation of two different control strategies for the multi-source generator permits to highlight the benefits of a smart regulation on seasonal and annual performance and, thus, to evaluate the competitiveness of this technology.

2. Building characteristics and climatic data

In order to compare the performance of the different heat pump configurations, a single-storey house [15] has been coupled to the heat pump system. The residential building, located in Bologna (Emilia-Romagna region, Northern Italy, 44°29'N, 11°21'E), has four thermal zones and a non-heated attic. The total net floor area is 111.6 m^2, the net conditioning volume is 301.5 m^3 and the surface to volume ratio is equal to 1.32 m^{-1}. The building main geometrical characteristics are summed up in Table 1, where the external wall surface area, the net floor area and the net volume are indicated for every thermal zone. Moreover, in each thermal zone the infiltration rate has been set to 0.5 vol h^{-1}. In Table 2 the building envelope thermophysical properties are reported.

Table 1. Main geometrical characteristics of each thermal zone

	Zone 1	Zone 2	Zone 3	Zone 4	Non heated-Attic
External wall surface area [m^2]	29.9	32.9	39.0	36.0	107.2
Net floor area [m^2]	18.6	24.8	37.2	31.0	113.9
Net volume [m^3]	50.2	67.0	100.5	83.8	269.1

The insulation level is medium if compared to the current Emilia-Romagna region transmittance limits [18]. The clear components are low-emissivity (equal to 0.1) double glasses (4/12/4) filled with Argon, with a glass transmittance of 1.5 W m^{-2} K^{-1}. The frame transmittance is 2 W m^{-2} K^{-1} and covers 20% of the total window surface. The standards UNI EN ISO 6949 [19] and UNI EN ISO 13370 [20] have been followed to calculate the external opaque components and the slab on grade transmittance values, respectively. Moreover, occupancy and equipment heat gains have not been considered.

The peak heating load is equal to 6.15 kW, whilst the maximum cooling load is 1.66 kW. The heating to cooling load ratio is equal to 3.7, thus, the building loads are strongly unbalanced, with higher values during the winter season. The thermal building loads have been evaluated by means of the ALMABuild tool by setting the indoor set-point temperature equal to 20 °C during winter and to 26 °C during summer. The heating season starts on October 15th and ends on April 30th (198 days), while the cooling season goes from June 15th to August 31st (77 days). The hourly climatic data included in the Meteonorm database [21] have been used in the dynamic simulations (minimum and maximum outdoor air temperature equal to -7 in winter and 35 °C in summer, respectively).

Table 2. Main characteristics of the opaque and clear components

	External wall	Floor	Roof	Window
Thickness [m]	0.34	0.335	0.32	0.02
Insulation thickness [m]	0.06	0.06	0.08	-
Transmittance [W m^{-2} K^{-1}]	0.38	0.28	0.401	1.77
Transmittance limits [W m^{-2} K^{-1}]	0.28	0.29	0.24	1.4

3. HVAC system characteristics

3.1. Sizing of the heat pump

The HVAC system, coupled to the building described above, is based on a single reversible inverter-driven heat pump. No back-up system is present because the heat generator has been sized to cover the maximum heating and cooling loads. To satisfy the building energy demand, three different heat pump systems have been considered: (i) an Air-Source Heat Pump, ASHP (air-to-water); (ii) a Ground-Coupled Heat Pump, GCHP (brine-to-water); (iii) a Dual-Source Heat Pump, DSHP (air/brine-to-water). As mentioned before, the DSHP is able to exploit, alternately, renewable energy from ambient air and soil, depending on the selected control strategy (no parallel exploitation of external sources is possible due to the unit refrigerant circuitation). The GCHP and ASHP manufacturer data on thermal power (cooling *Pc* and heating capacity *Ph*), COP and EER are reported in Figures 1 and 2 for different values of the external source temperature and different inverter frequencies. The curves refer to a load water temperature at the heat pump outlet equal to 10 °C in summer and 40 °C in winter. The DSHP has been modelled by considering the characteristic curves of both the ASHP and the GCHP.

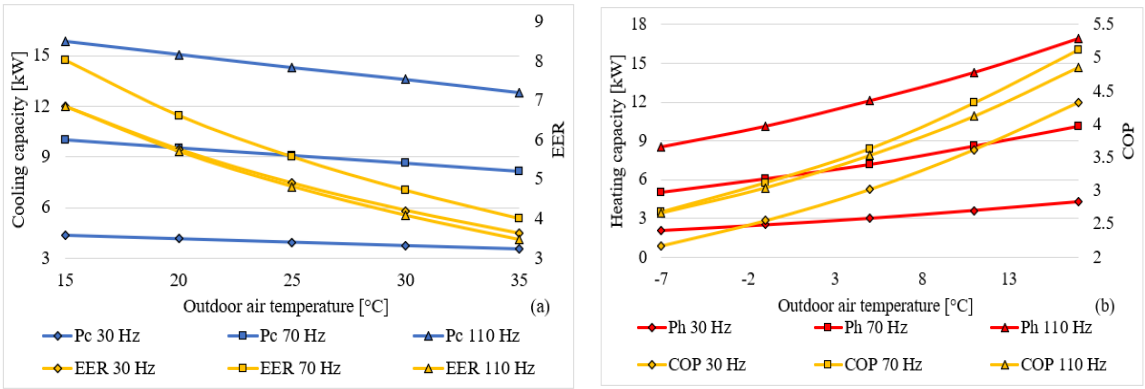

Fig. 1. (a) Cooling capacity and EER and (b) heating capacity and COP as functions of the outdoor air temperature (air-source mode), for three values of the inverter frequency (30 Hz, 70 Hz, 110 Hz).

The selected GCHP and ASHP can satisfy 1.45 and 1.38 times, respectively, the building heating peak load in the most unfavourable conditions (borehole fluid temperature of -5 °C in ground-source mode and external air temperature of -7 °C in air-source mode). Since the building winter energy demand is the most relevant, during summer the heat pump is deeply oversized and this will implicate a large number of on-off cycles.

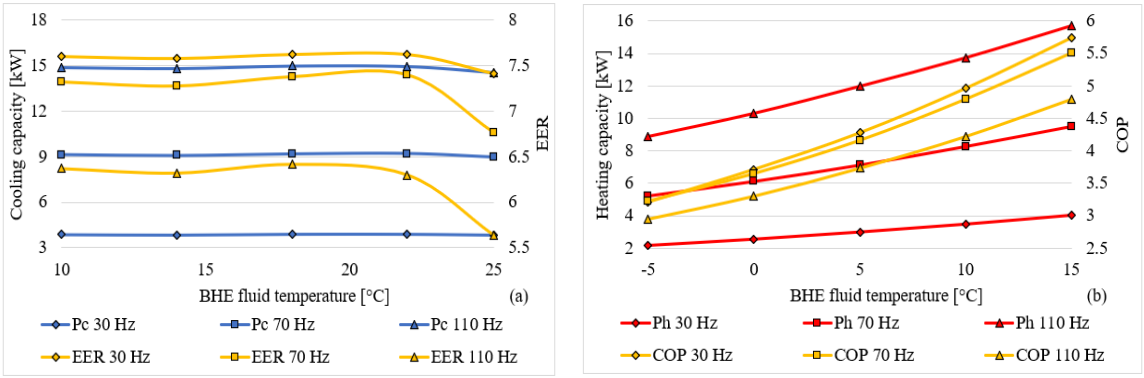

Fig. 2. (a) Cooling capacity and EER and (b) heating capacity and COP as functions of the borehole fluid temperature at the heat pump inlet (ground-source mode), for three values of the inverter frequency (30 Hz, 70 Hz, 110 Hz).

3.2. Heat pump control system

A PI controller is necessary to regulate the heat pump inverter frequency based on the temperature of the water supplied to the emitters. According to the hysteresis cycle adopted, the heat pump is switched off when the water temperature exceeds/goes under 42.5/7.5 °C and switched on when the water temperature decreases below/increases over 37.5/12.5 °C in winter and summer, respectively. When the minimum inverter frequency (30 Hz) is reached, no further thermal capacity modulation is possible, so the heat pump has to perform on-off cycles to satisfy the building thermal energy demand. In addition, the heat pump in air-source mode has to perform defrost cycles when the outdoor air temperature is low and the relative humidity is high.

In order to evaluate the energy losses linked to on-off and defrost cycles, corrective coefficients of the heat pump performance data have been applied. Concerning the on-off cycles, two coefficients have been used [15]. The first one, α, is related to the reduction of the thermal power supplied by the heat pump during the transient start-up of duration τ_α. The second one, β, is related to the reduction of the electric power requested by the heat pump during the transient start-up of duration τ_β. The correct thermal and electric power values have been obtained by multiplying the nominal ones to the corresponding corrective coefficients for the whole transient start-up duration. The values of the penalty coefficients (α, β) and the transient start-up times (τ_α, τ_β) are reported in Table 3.

Table 3. Penalty coefficients and transient start-up time

α	β	τ_α [s]	τ_β [s]
0.69	0.96	216	78

The heat pump cycle inversion due to defrosting occurs when, at the same time and for at least 10 minutes, the outdoor air temperature is lower than 6 °C and the relative humidity is higher than 50%. To model the defrost cycles, three phases have been considered [7]: i) an initial phase τ_1 in which the heat pump is switched-off and the inversing valve is turned on; (ii) an intermediate phase τ_2 during which the cycle is inverted and the heat pump operates in cooling mode, with power P_c and efficiency EER_c; (iii) a final phase τ_3 in which the heat pump is switched-off and the inversing valve is reverted again, to return in heating mode. One hour must pass between two consecutive defrost cycles. Table 4 shows the adopted values of P_c, EER_c, τ_1, τ_2 and τ_3.

Table 4. Main characteristics of the defrost cycle

P_c [kW]	EER_c	τ_1 [s]	τ_2 [s]	τ_3 [s]
-11.4	6	30	360	30

In order to select the most favorable external source (air/ground) when a DSHP is considered, two different control strategies have been analyzed: the switching temperature logic and the scheduled times logic. In the

former, when the external air temperature exceeds a reference value, called switching temperature, the heat pump operates in air-mode, otherwise it operates in ground-mode. In the latter, two daily scheduled time slots, nocturnal and diurnal, have been considered, taking as time limits the monthly average hours of sunrise and sunset in Bologna [22], reported in Table 5. In the diurnal hours the heat pump exploits the aerothermal energy, whereas in the nocturnal hours it uses the geothermal energy.

Four different case studies have been considered: heat pump system based on a GCHP (case A), heat pump system based on an ASHP (case B), heat pump system based on a DSHP with switching temperature logic (case C), heat pump system based on a DSHP with scheduled times logic (case D).

Table 5. Sunrise and sunset monthly average hours in Bologna

	Jan	Feb	Mar	Apr	May	Jun	Jul	Aug	Sep	Oct	Nov	Dec
Sunrise [a.m. h]	7:26	6:52	6:10	5:23	4:43	4:23	4:32	5:07	5:52	6:38	7:17	7:37
Sunset [p.m. h]	4:34	5:08	5:50	6:37	7:17	7:37	7:28	6:53	6:08	5:22	4:43	4:23

3.3. Terminal units and BHE field

In each case study, fan-coils are considered as emitters, that are connected to the heat pump through a hydronic loop where a single-speed circulation pump is present. The HVAC system is activated 24/24 h both during the heating and the cooling season. In order to reduce the heat pump on-off cycles and the thermal zones discomfort during defrost cycles, an inertial tank of 500 l has been placed in the heat pump delivery pipe.

The three-speed fan-coils selected, operating with a constant water flow rate, have been sized to cover the thermal zones load considering an inlet water temperature of 40 and 10 °C in the heating and cooling season, respectively. The fan controller modulates the speed (off, low, medium, or high) based on the room temperature, in order to maintain the set point value of 20 °C in winter and 26 °C in summer. When the fan is switched off, the water flow rate by-passes the terminal unit thanks to a three-way valve. Table 6 reports the fan-coils technical data of air and water flow rate, heating and cooling capacity, in correspondence of the indoor air temperature T_{amb}, inlet/outlet water temperature T_{in}/T_{out}, fan speed *fs* and relative humidity *RH*.

Table 6. Fan-coils technical data. Seasonal reference conditions: T_{amb} =20 °C, T_{in}/T_{out} =40/35 °C, high *fs* in heating mode; T_{amb} =26 °C, T_{in}/T_{out} =10/15 °C, medium *fs* and *RH* 60% in cooling mode

	Zone 1	Zone 2	Zone 3	Zone 4
Air flow rate [$m^3\ h^{-1}$]	442 [1] – 341 [2]	442 [1] – 341 [2]	319 [1] – 233 [2]	319 [1] – 233 [2]
Water flow rate [$l\ h^{-1}$]	253	253	158	317
Heating capacity [W]	1890	1890	1170	1410
Cooling capacity [W]	1540	1540	900	1330

[1] Heating mode

[2] Cooling mode

When the heat pump works in ground-mode (cases A, C, D), another hydronic loop with a single-speed circulation pump connects the heat pump to a BHE field. In Figure 3 a simplified HVAC layout with the multi-source heat pump is shown.

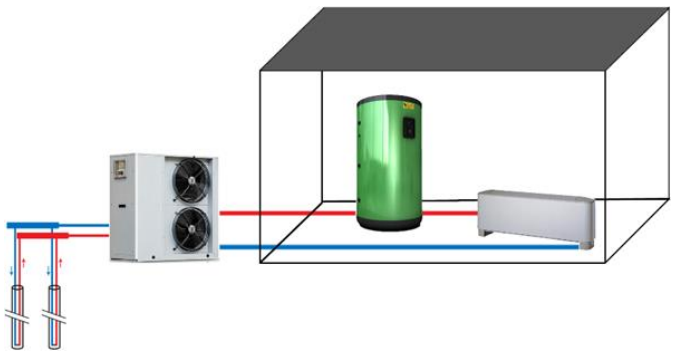

Fig. 3. Simplified HVAC layout with the multi-source heat pump.

The BHE field coupled to the heat pump contains vertical single U-tube boreholes, made of high-density polyethylene pipes in which a mixture of water and 60% Freezium [23] flows. Freezium is a commercial antifreeze borehole fluid, based on organic salts (potassium formate), able to maintain low viscosity and high thermal conductivity in low temperature applications. The gap between U-tubes and ground is filled by a commercial sealant mortar (Termoplast Plus [24]). The main BHE characteristics (borehole diameter D_b, internal pipe diameter $D_{p,i}$, external pipe diameter $D_{p,e}$, grout conductivity k_{gt}, pipe conductivity k_p, shank spacing s, BHE fluid thermal conductivity k_f, kinematic viscosity v_f and freezing temperature T_{ice}) are reported in Table 7.

Table 7. BHE and borehole fluid characteristics

D_b [m]	$D_{p,i}$ [m]	$D_{p,e}$ [m]	k_{gt} [W m^{-1} K^{-1}]	k_p [W m^{-1} K^{-1}]	s [m]	k_f[1] [W m^{-1} K^{-1}]	v_f[1] [m^2 s^{-1}]	T_{ice} [°C]
0.13	0.0262	0.032	1.6	0.355	0.085	0.5	2.2E-6	-25

[1]Property at 0 °C.

The undisturbed ground temperature has been set equal to 13.2 °C, whilst the ground thermal conductivity and diffusivity have been set as 1.97 W m^{-1} K^{-1} and 8.8E-7 m^2 s^{-1}, respectively. The borehole thermal power per unit length, exchanged between BHEs and ground, ranges between 30 and 50 W m^{-1} [25-26]. The borefield in case A (GCHP) is made of 2 BHEs, each 60 m long. For case C (DSHP with switching temperature logic), 4 different borefield configurations have been considered: 2 boreholes each 60 m long (case C1); 1 borehole 90 m long (case C2); 1 borehole 70 m long (case C3); 1 borehole 60 m long (case C4). In cases C2-C4 the total BHEs length is undersized with respect to the building energy demand. Finally, in case D (DSHP with scheduled times logic) only 1 borehole 60 m long has been considered. Table 8 sums up the different case studies.

Table 8. Sum up of the case studies

	A	B	C1	C2	C3	C4	D
Ground	2×60 m	×	2×60 m	1×90 m	1×70 m	1×60 m	1×60 m
Air	×	✓	✓	✓	✓	✓	✓

The ground thermal response has been modeled by means of the *g-functions* method, in which dimensionless thermal response functions simulate the ground temperature trend produced by a uniform and constant dimensionless thermal load [27]. By means of *g-functions*, the BHE fluid outlet temperature has been evaluated at every simulation time step [9], whilst the BHE linear thermal resistance has been calculated with an analytical expression [28].

4. Results

The entire system has been modelled in ALMABuild, a homemade tool developed in the Matlab-Simulink environment for the dynamic simulation of coupled building-HVAC plants [16-17]. ALMABuild contains libraries with blocks to model the different building and HVAC components. The considered system, shown in Figure 4, has been modelled by using blocks from both ALMABuild and Carnot, another Simulink library focused on the HVAC system [29].

Yearly and long-term (7 years) simulations have been carried out to investigate the performance of the considered heat pump systems on the basis of the seasonal and annual efficiency indicators reported in Equation (1). In order to limit the computational time of performed simulations with no lack of reliability, a period of 7 years has been considered idoneous to investigate the (eventual) soil temperature drift, since the variation of the ground temperature stabilizes in a few years for all configurations presented in this paper.

$$SCOP_{net} = \frac{\sum_{j=0}^{\tau_h} E_{h,j}}{\sum_{j=0}^{\tau_h} E_{el,j}} \qquad SEER = \frac{\sum_{j=0}^{\tau_c} E_{c,j}}{\sum_{j=0}^{\tau_c} E_{el,j}} \qquad APF_{net} = \frac{\sum_{j=0}^{\tau_h+\tau_c} E_{h,j} + E_{c,j}}{\sum_{j=0}^{\tau_h+\tau_c} E_{el,j}} \tag{1}$$

The net Seasonal Coefficient of Performance ($SCOP_{net}$) is the winter performance indicator, namely the ratio between the total thermal energy provided by the heat pump during winter $\left(\sum_{j=0}^{\tau_h} E_{h,j}\right)$ and the

corresponding electric energy used by the heat pump compressor $\left(\sum_{j=0}^{\tau_h} E_{el,j}\right)$. The Seasonal Energy Efficiency Ratio (SEER) is the summer performance indicator, that is the ratio between the total cooling energy provided by the heat pump during summer $\left(\sum_{j=0}^{\tau_c} E_{c,j}\right)$ and the corresponding electric energy used by the heat pump compressor $\left(\sum_{j=0}^{\tau_c} E_{el,j}\right)$. The net Annual Performance Factor (APF_{net}) is the annual performance indicator, i.e., the ratio between the total energy supplied by the heat pump during the year $\left(\sum_{j=0}^{\tau_h+\tau_c} E_{h,j} + E_{c,j}\right)$ and the corresponding total electric energy used $\left(\sum_{j=0}^{\tau_h+\tau_c} E_{el,j}\right)$.

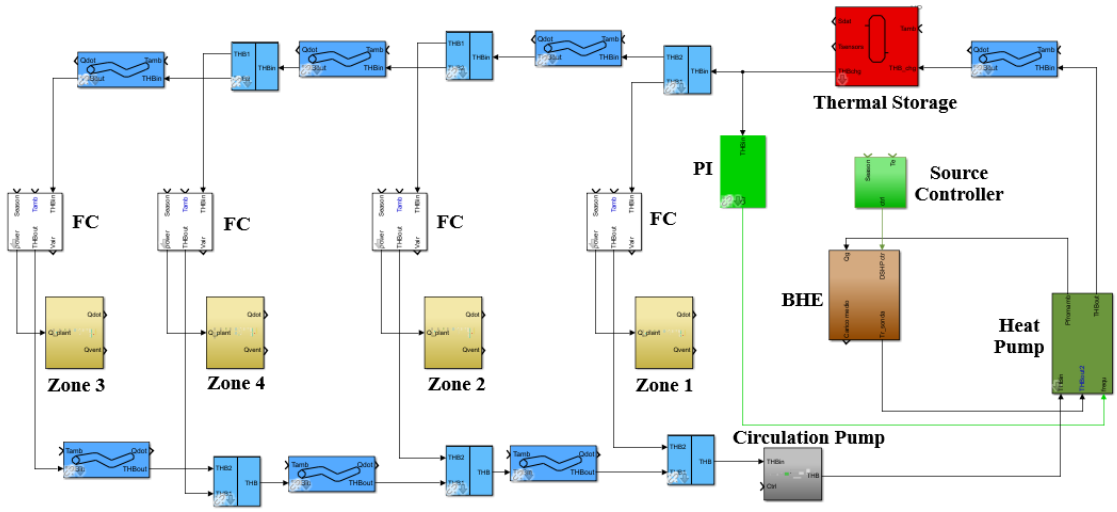

Fig. 4. Building-HVAC system layout (Borehole Heat Exchanger BHE, Proportional Integral controller PI, Fan-coil FC).

4.1. Case A, GCHP

In case A, the GCHP is coupled to the single-storey house and to the BHE field with 2 boreholes, each 60 meters long. The long-term heat pump performance and ground temperature trend have been evaluated. In Table 9 the seasonal and annual performance factors obtained from the first to the 7th year are reported together with the percent variation on the APF_{net} value (Δ_{APF}) with respect to the first year, taken as reference.

Table 9. Seasonal and annual performance factors, GCHP

Year	1	2	3	4	5	6	7
SEER	6.24	6.23	6.23	6.23	6.23	6.23	6.23
$SCOP_{net}$	3.95	3.89	3.86	3.84	3.83	3.82	3.81
APF_{net}	4.07	4.01	3.98	3.96	3.94	3.93	3.93
Δ_{APF} [%]	0	-1.45	-2.17	-2.64	-2.98	-3.24	-3.43

As evident from Table 9, the best efficiency is reached in the cooling season due to an oversized borefield, which allows to keep the maximum BHE fluid temperature at the heat pump inlet below 20 °C. On the contrary, in the heating season the BHE field is well-sized and the seasonal performance ($SCOP_{net}$) remains quite high over the years, with a maximum value of 3.95 in correspondence of the first year. The APF_{net} index follows the $SCOP_{net}$ trend over the 7-years period because the building loads are strongly unbalanced with predominance of the heating demand. Furthermore, it can be observed that the minimum APF_{net} value, obtained at the last year, is only 3.43% lower than that of the first year. This result is explained by the mean winter temperature values at the BHE-ground interface, which drop only slightly over the years, going from 5.7 °C (first year) to 4.35 °C (seventh year). On the contrary, in presence of both unbalanced building loads and undersized borefield, the ground thermal drift can be significant [27].

4.2. Case B, ASHP

In case B, the ASHP is coupled to the same residential building. Since Meteonorm hourly climatic data refer to a typical reference year, one annual simulation is sufficient to investigate the generator efficiency in the long-term period. In Table 10 the seasonal and annual performance indicators are reported.

Table 10. Seasonal and annual performance factors, ASHP

SEER	$SCOP_{net}$	APF_{net}
4.06	2.80	2.87

From Table 10 it can be observed that the minimum seasonal efficiency refers to the winter season: the $SCOP_{net}$ value is equal to 2.80, about 31% lower than the SEER value (4.06). This result is due to the high number of heat pump start-ups: 2873 over the year, where 2547 start-ups occur during the winter period and only 326 during the summer one. The large number of winter start-ups mainly depends on the defrost cycles, which are about 9 per day. This aspect becomes even more critical in the coldest and damp months, from December to February, when the daily average number of defrost cycles overcomes 15. In the summer season the heat pump is often switched off (79% of the conditioning period), given that the cooling demand is much lower than the heating one, so that the generator is deeply oversized during this season. Indeed, the maximum compressor frequency does not overcome 39 Hz during the cooling season (the heat pump frequency range goes from 30 to 110 Hz). The APF_{net} value (2.87) is close to the winter coefficient (2.80), due to the unbalanced building loads.

4.3. Cases C1-C4, DSHP with switching temperature logic

In cases C1-C4, the heat pump is a DSHP able to exploit, alternatively, renewable energy from both air and ground. In the heating season, the adopted source control strategy is the switching temperature logic: the controller compares the ambient temperature with a reference value (switching temperature). In particular, when the external air temperature exceeds the switching temperature, the heat pump operates in air-mode, otherwise in ground-mode. In this way the aerothermal energy can be used when the outdoor air temperature is warmer (with consequent higher COP values) and the defrost cycles can be avoided if a switching temperature higher than 6 °C is selected. On the other hand, in the cooling season the heat pump works in ground-mode only in order to partially recharge the ground due to the unbalanced building loads and to exploit a sink with lower temperature values than the external air, with consequent better EER values.

In case studies C1-C4, 4 different BHE sizes have been coupled to the multi-source heat pump. Figure 5 shows the first year APF_{net} trend as a function of the switching temperature, for the different BHE field lengths. It is worth noting that a switching temperature equal to 26 °C (points on the far right in Figure 5) corresponds to ground-source mode only, namely to a conventional GCHP. From Figure 5 it can be observed that the APF_{net} increases, for a fixed switching temperature, ranging from case C4 (BHE length 60 m) to cases C3 (BHE length 70 m), C2 (BHE length 90 m) and C1 (BHE length 120 m). Indeed, the higher the total BHE length, the higher (the lower) the BHE fluid temperature at the heat pump inlet and, consequently, the better the heat pump winter (summer) performance.

Another important obtained outcome is that an optimal switching temperature can be selected, for a fixed BHE length, that maximizes the APF_{net} value. In particular, this optimal value grows as the borefield length rises: in cases C3 and C4 (shorter borefields) the optimal switching temperature is 6 °C, whereas in cases C2 and C1 (longer borefields) it becomes 8 and 14 °C, respectively. This trend is coherent since the ground utilization increases with the switching temperature, and longer BHEs guarantee higher (lower) borehole fluid temperature values, assuring better heating (cooling) performance. By comparing the results of cases C3 and C4 to each other, it is clear that the adoption of an optimized switching temperature allows to achieve, with a shorter borefield, the same APF_{net} value of a conventional GCHP coupled to a longer (and more expensive) field: the APF_{net} value for case C4 (BHE 60 m long) in correspondence of a switching temperature T_{sw} = 6 °C is 8% larger than that in correspondence of T_{sw} =26 °C (ground-source mode only) and even slightly larger than that achieved in case C3 (BHE 70 m long) with T_{sw} =26 °C (ground-source mode only). Moreover, adopting a switching temperature of 14 °C even in the well-sized case C1 allows to obtain an APF_{net} slightly greater than that of the traditional GCHP (T_{sw} = 26 °C). Indeed, with T_{sw} = 14 °C, the air source is employed when the external air temperature is higher than the ground temperature and this promotes better heat pump performance (compare the heat pump performance data in Figures 1 and 2). Small switching temperature

values can be discarded as they make the heat pump operate for a prolongated time with the aerothermal source even when the ambient temperature is cold and dump.

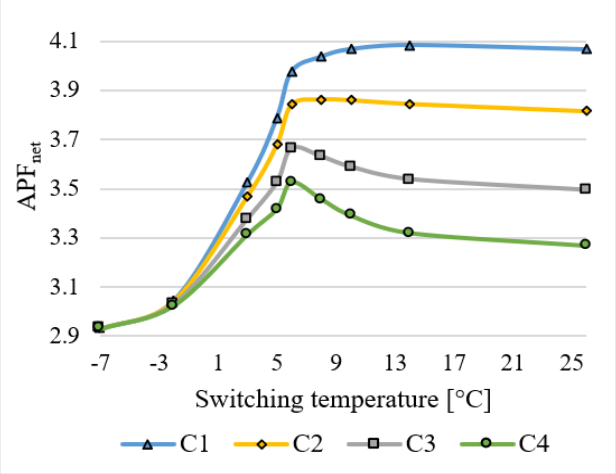

Fig. 5. First year APF_{net} as function of the switching temperature and of the BHE field size (C1, C2, C3, and C4).

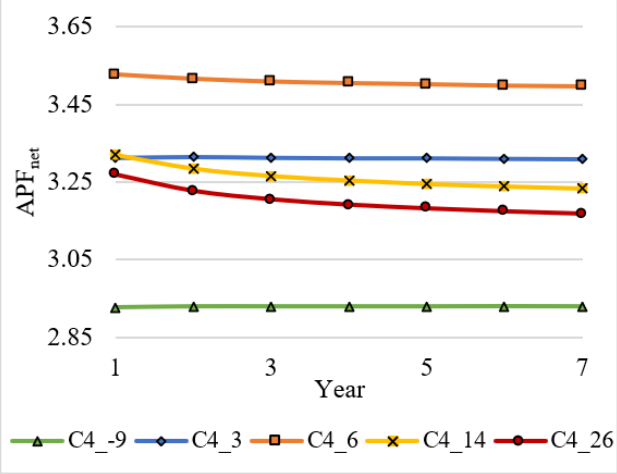

Fig. 6. APF_{net} trend of case C4 over 7 years, for different switching temperature values (-9, 3, 6, 14 and 26 °C).

In order to evaluate the long-term heat pump performance, 7-years simulations have been carried out by coupling the DSHP to the most undersized borefield, namely case C4 (1×60 m). Five switching temperature values (-9, 3, 6, 14, 26 °C) have been selected and the corresponding annual efficiency is reported in Figure 6. It is worth remembering that a switching temperature of 26 °C (red curve in Figure 6) corresponds to simulate a conventional GCHP. It can be observed from Figure 6 that the DSHP APF_{net} with a very low switching temperature (T_{sw} = -9 °C, green curve) has a steady trend since no ground energy is exploited in winter and, therefore, no ground temperature degradation occurs. Additionally, the thermal energy transferred to the ground in the cooling season is insufficient to markedly increase its temperature over the years, thus no influence on the SEER values has been noticed.

On the other hand, the DSHP APF_{net} with a very high switching temperature (T_{sw} = 26 °C, red curve) is always higher than that obtained with T_{sw} = -9 °C, but the ground temperature degradation negatively influences the annual efficiency, which has a drop of 3.1% after 7 years.

As already mentioned before, the optimal switching temperature for case C4 is 6 °C (orange curve in Figure 6): adopting this control logic, the thermal energy extracted in winter from ground decreases by 40% compared to the GCHP case (red curve). As a consequence, the mean winter temperature of the BHE fluid at the DSHP inlet is from 6.6 °C (1st year) to 7.3 °C (7th year) higher than that reached in the same year by the GCHP and the APF_{net} increases from 8 to 10.4% over the considered period.

Therefore, in accordance with the literature results [15, 30-31], the adoption of a DSHP proves to be competitive: (i) to equilibrate the ground loads when the building loads are strongly unbalanced and/or when the borefield is undersized, avoiding the progressive ground temperature drift; (ii) to reduce the HVAC plant investment cost opting for a total BHE field length reduced with respect to the design one.

4.4. Case D, DSHP with scheduled times logic

In case D, the heat generator is composed of a dual-source heat pump coupled to an undersized (60-meters long) borehole. In the heating season the source control strategy is the scheduled times logic: two daily scheduled time slots, nocturnal and diurnal, are defined taking as time limits the monthly average hours of sunrise and sunset in Bologna. In the diurnal hours the heat pump exploits aerothermal energy and in the nocturnal ones geothermal energy. With this control logic the number of defrost cycles depends on the temperature and moisture content of the external air in the diurnal hours. On the other hand, in the cooling season the source controller selects only the ground for the same reasons explained for the switching temperature logic (section 4.3). Table 11 shows the results in terms of seasonal and annual performance coefficients over 7 years. As evident from Table 11, the best seasonal efficiency is reached in summer due to a well-sized borefield, with a mean summer BHE fluid temperature at the heat pump inlet which remains below 17.3 °C over the years. On the contrary, in the heating season the BHE field length is halved with respect to the proper design size and the $SCOP_{net}$ values are 48% lower than the SEER ones. Also in this case the APF_{net} index follows the $SCOP_{net}$ trend over the 7-years period because of the higher building loads for heating. Both

the $SCOP_{net}$ and the APF_{net} factors are quite stable over the years, undergoing a weak decrease, due to the mean winter temperature at the BHE-ground interface which drops from 4.7 °C (first year) to 4 °C (seventh year).

Table 11. Seasonal and annual performance factors, DSHP with scheduled times logic

	1	2	3	4	5	6	7
SEER	6.23	6.23	6.23	6.23	6.24	6.24	6.24
$SCOP_{net}$	3.26	3.25	3.25	3.24	3.24	3.23	3.23
APF_{net}	3.38	3.37	3.37	3.36	3.36	3.36	3.35

4.5. Comparison

The main results in terms of APF_{net} for the investigated cases A-D are summed up in Figure 7.

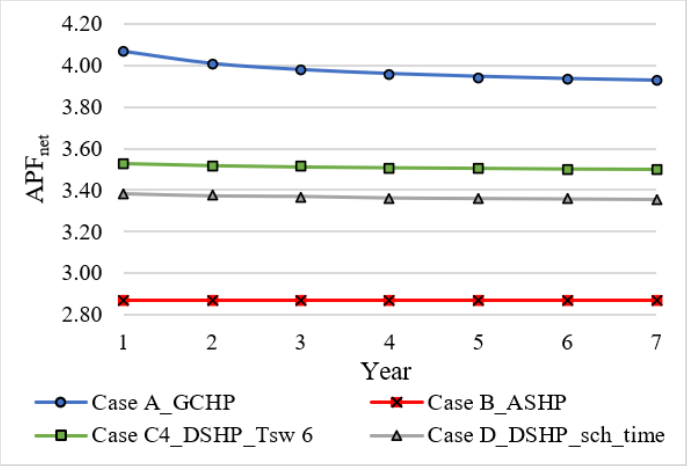

Fig. 7. APF_{net} over 7 years of cases A (blue curve), B (red curve), C4 (green curve) and D (grey curve).

According to the plot of Figure 7, the best annual efficiency is reached adopting a traditional GCHP (blue curve in Figure 7) coupled to a well-sized borefield (case A). In this case, the APF_{net} index drops slightly, especially in the first three years, reaching a value of 3.94 after 7 years. The worst performance is obtained by the ASHP (case B, red curve in Figure 7) due to a colder source in winter and to a large number of defrost cycles. The performance of the DSHP coupled to a strongly undersized borefield (1×60 m) is intermediate between that of cases A and B, with the APF_{net} of the C4 configuration with T_{sw}=6 °C (green curve in Figure 7) 4% better than that of the D one (scheduled times logic, grey curve in Figure 7). This result is due to a better exploitation of the renewable sources in case C4: in the scheduled times logic (case D) the number of defrost cycles cannot be controlled because it depends on the temperature and moisture content of the outdoor air in the diurnal hours (when the heat pump operates in air-mode), whereas the switching temperature logic with an optimized T_{sw} (case C4) avoids the inefficient defrost cycles making the heat pump operate in ground-source mode when the external air temperature is below 6 °C. In both cases C4 and D the APF_{net} is quite stable over the seven years thanks to more balanced ground loads with respect to case A. To summarize, the DSHP guarantees an annual efficiency from 17 to 23% larger than that obtained by a conventional ASHP, independently from the logic chosen to select the operating external source. Furthermore, accepting an APF_{net} value only 11% lower with respect to case A, a borefield strongly reduced up to 50% can be coupled to the DSHP, obtaining, in this way, a consistent reduction of the investment cost.

5. Conclusion

In this paper, the homemade Simulink-MATLAB tool ALMABuild has been employed to investigate the performance of different heat pump systems, coupled to the same single-storey house, located in Bologna (North Italy) and characterized by unbalanced seasonal loads. Three heat pump configurations have been considered: a Ground-Coupled Heat Pump (GCHP), an Air-Source Heat Pump (ASHP) and a Dual-Source Heat Pump (DSHP), modelled through the technical data of both the ASHP and the GCHP. In dual-source

mode two different control strategies have been tested: the switching temperature logic and the scheduled times one. In the former, when the external air temperature exceeds a reference value, called switching temperature, the heat pump operates in air-mode, otherwise in ground-mode. In the latter, two daily scheduled time slots, nocturnal and diurnal, have been considered taking as time limits the monthly average hours of sunrise and sunset in Bologna; in the diurnal hours the heat pump exploits aerothermal energy, in the nocturnal hours the heat pump extracts heat from the ground.

Yearly and long-term (7 years) simulations have been carried out to investigate the different heat pump systems performance. The numerical results demonstrate that, when the borefield is well-sized, the DSHP performance is higher than that of the ASHP and lower than that of the GCHP. Moreover, with the switching temperature logic an optimal value can be adopted to maximize the APF_{net}; the optimal switching temperature value rises as the BHE field length increases. Additionally, in presence of undersized BHEs, annual performance factors higher than that of a GCHP can be obtained by a DSHP with an optimized switching temperature, with a consistent reduction of the borefield investment cost. Furthermore, with the scheduled times logic, lower APF_{net} values are obtained compared to those of the switching temperature logic due to a worst sources selection. More balanced ground loads are guaranteed by the multi-source heat pump, resulting in more stable APF_{net} values than those of the GCHP over the years. The adoption of a DSHP is promising since it allows to reduce the ground temperature drift originated by an undersized borefield and/or unbalanced building loads. As a consequence, DSHPs can be selected for the replacement of conventional GCHPs in presence of BHEs that are undersized (to reduce the investment cost or due to subsequent changes in the building thermal loads).

Acknowledgements

The research leading to these results has received funding from the Italian Ministry of University and Research (MUR) within the framework of the PRIN2017 project «The energy FLEXibility of enhanced HEAT pumps for the next generation of sustainable buildings (FLEXHEAT)», grant 2017KAAECT.

References

[1] E.U. Directive 2018/2002/EU on Energy Efficiency, amending Directives 2012/27/EU, 2009/12/EC and 2010/30/EU and repealing Directives 2004/8/EC and 2006/32/EC, 21 December 2018.
[2] E.U. Directive 2018/844/EU of the European Parliament and of the Council amending Directive 2010/31/EU on the energy performance of buildings and Directive 2012/27/EU on energy efficiency, 30 May 2018.
[3] MISE, Annual Energy Report, 22 July 2021.
[4] MISE, Requirement to obtain tax deduction for building energy upgrading, 6 August 2020.
[5] Madonna F, Bazzocchi F. Annual performances of reversible air-to-water heat pumps in small residential buildings. *Energy and Buildings* 2013;**65**:299–309.
[6] Dongellini M, Naldi C, Morini GL. Seasonal performance evaluation of electric air-to-water heat pump systems. *Applied Thermal Engineering* 2015;**90**:1072–81.
[7] Vocale P, Morini GL, Spiga M. Influence of outdoor air conditions on the air source heat pumps performance. *Energy Procedia* 2014;**45**:653–62.
[8] Urchueguía JF, Zacarés M, Corberán JM, Montero Á, Martos J, Witte H. Comparison between the energy performance of a ground coupled water to water heat pump system and an air to water heat pump system for heating and cooling in typical conditions of the European Mediterranean coast. *Energy Conversion and Management* 2008;**49**:2917–23.
[9] Naldi C, Zanchini E. Effects of the total borehole length and of the heat pump inverter on the performance of a ground-coupled heat pump system. *Applied Thermal Engineering* 2018;**128**:306–19.
[10] Rivoire M, Casasso A, Piga B, Sethi R. Assessment of Energetic, Economic and Environmental Performance of Ground-Coupled Heat Pumps. *Energies* 2018;**11**:1941. doi:10.3390/en11081941
[11] Kaygusuz K, Ayhan T. Experimental and theoretical investigation of combined solar heat pump system for residential heating. *Energy Conversion & Management* 1999;**40**:1377–96.
[12] Lazzarin RM. Dual source heat pump system: Operation and performance. *Energy and Buildings* 2012;**52**:77–85.
[13] Fu HD, Pei G, Ji J, Long H, Zhang T, Chow TT. Experimental study of a photovoltaic solar-assisted heat-pump/heat-pipe system. *Applied Thermal Engineering* 2012;**40**:343–50.

[14] Ammar AA, Sopian K, Alghoul MA, Elhub B, Elbreki AM. Performance study on photovoltaic/thermal solar-assisted heat pump system. *J Therm Anal Calorim* 2019;**136**:79–87. https://doi.org/10.1007/s10973-018-7741-6
[15] Grossi I, Dongellini M, Piazzi A, Morini GL. Dynamic modelling and energy performance analysis of an innovative dual-source heat pump system. *Applied Thermal Engineering* 2018;**142**:745–59.
[16] Campana JP. ALMABEST: A new whole building energy simulation Simulink-based tool for NZEB design (PhD dissertation, Supervisor: Gian Luca Morini). Alma Mater Studiorum - University of Bologna 2019. doi: 10.6092/unibo/amsdottorato/8993
[17] Campana JP, Morini GL. BESTEST and EN ISO 52016 Benchmarking of ALMABuild, a New Open-Source Simulink Tool for Dynamic Energy Modelling of Buildings. *Energies* 2019;**12**:2938. doi:10.3390/en12152938
[18] Dgr Emilia-Romagna. Modifications acceptance to "Deed of regional technical coordination to define energy performance and minimum requirements of buildings, n.967/2015". July 2022.
[19] UNI EN ISO 6946:2008 Building Components and Building Element - Thermal Resistance and Thermal Transmittance - Calculation Method.
[20] UNI EN ISO 13370:2018 Thermal performance of buildings - Heat transfer via the ground - Calculation methods.
[21] METEONORM. Global Meteorological Database for Solar Energy and Applied Climatology. Available: http://www.meteonorm.com
[22] UNI 10349-1:2016 Heating and cooling of buildings - Climatic data – Part 1: Monthly means for evaluation of energy need for space heating and cooling and methods for splitting global solar irradiance into the direct and diffuse parts and for calculate the solar irradiance on tilted planes.
[23] Gernot Krakat. *VDI Heat Atlas.* 2sd ed. Mülheim (Ruhr): Springer D4.2 p 451; 2010.
[24] Termoplast PLUS, pre-mixed for the filling of geothermal weels, technical datasheet. Available: https://www.gtssnc.com/schedetecniche/premiscelato_Termoplast_PLUS.pdf
[25] Lee CK, Lam HN. Computer simulation of borehole ground heat exchangers for geothermal heat pump systems. *Renewable Energy* 2008;**33**:1286–96.
[26] Florides G, Kalogirou S. Ground heat exchangers – A review of systems, models and application. *Renewable Energy* 2007;**32**:2461–78.
[27] Zanchini E, Lazzari S. Temperature distribution in a field of long Borehole Heat Exchangers (BHEs) subjected to a monthly averaged heat flux. *Energy* 2013;**59**:570–80.
[28] Lamarche L, Kajl S, Beauchamp B. A review of methods to evaluate borehole thermal resistances in geothermal heat-pump systems. *Geothermics* 2010;**39**:187–200.
[29] CARNOT Toolbox Ver. 7.0, 07/2019 for Matlab/Simulink R2018b, © Solar-Institut Juelich.
[30] Corberán JM, Cazorla-Marín A, Marchante-Avellaneda J, Montagud C. Dual source heat pump, a high efficiency and cost-effective alternative for heating, cooling and DHW production. *International Journal of Low-Carbon Technologies* 2018;**13**:161–76.
[31] Marinelli S, Lolli F, Butturi MA, Rimini B, Gamberini R. Environmental performance analysis of a dual-source heat pump system. *Energy & Buildings* 2020;223 110180.